

A GENUINELY MULTIDISCIPLINARY JOURNAL

CHEMPLUSCHEM

CENTERING ON CHEMISTRY

Accepted Article

Title: Graphitic Carbon Nitride (g-C₃N₄) Supported Pd Species: An Efficient Heterogeneous Photocatalyst Surpassing Homogeneous Thermal Heating Systems for Suzuki Coupling

Authors: Nan Wang, Lixia Ma, Jing Wang, Yanpei Zhang, and Ruibin Jiang

This manuscript has been accepted after peer review and appears as an Accepted Article online prior to editing, proofing, and formal publication of the final Version of Record (VoR). This work is currently citable by using the Digital Object Identifier (DOI) given below. The VoR will be published online in Early View as soon as possible and may be different to this Accepted Article as a result of editing. Readers should obtain the VoR from the journal website shown below when it is published to ensure accuracy of information. The authors are responsible for the content of this Accepted Article.

To be cited as: *ChemPlusChem* 10.1002/cplu.201900360

Link to VoR: <http://dx.doi.org/10.1002/cplu.201900360>

WILEY-VCH

www.chempluschem.org

A Journal of



Graphitic Carbon Nitride ($g\text{-C}_3\text{N}_4$) Supported Pd Species: An Efficient Heterogeneous Photocatalyst Surpassing Homogeneous Thermal Heating Systems for Suzuki Coupling

Nan Wang, Lixia Ma, Jing Wang, Yanpei Zhang, and Ruibin Jiang*

Abstract: Suzuki coupling reactions play a paramount importance in C–C coupling reactions. However, Suzuki coupling reactions are generally catalyzed by homogeneous catalysts under thermal heating, which imparts difficulty on the catalyst separation and consumes a relatively large amount of energy. Herein, $g\text{-C}_3\text{N}_4/\text{Pd}$ is successfully prepared for photocatalytic Suzuki coupling reactions. The $g\text{-C}_3\text{N}_4/\text{Pd}$ is prepared through the reduction of Pd source in the presence of $g\text{-C}_3\text{N}_4$. The Pd is found to exist as Pd nanoparticles and Pd(II) species on $g\text{-C}_3\text{N}_4$. Owing to the good light absorption of $g\text{-C}_3\text{N}_4$ and the excellent catalytic activity of Pd species, the $g\text{-C}_3\text{N}_4/\text{Pd}$ exhibits an excellent photocatalytic performance for Suzuki coupling reactions with TOF of 47.3 h^{-1} , which is almost two times of that of commercial homogeneous catalyst, $\text{Pd}(\text{PPh}_3)_4$, under thermal heating. Moreover, $g\text{-C}_3\text{N}_4/\text{Pd}$ displays very good recyclability and wide applicability for Suzuki coupling reactions. Our findings provide a green and sustainable way for the catalysis of Suzuki coupling reactions.

Suzuki coupling reaction provides an effective way to realize C–C coupling through an aryl halide and an aryl boronic acid.^[1–3] It is generally carried out at elevated temperature in the presence of homogeneous Pd-based compositions.^[1–3] Homogeneous catalysts impart difficulty on the separation of catalysts and products. Compared with homogeneous catalysts, heterogeneous catalysts can be easily separated from the reaction solutions through centrifugation. Therefore, many efforts have been devoted to developing heterogeneous catalysts for Suzuki coupling reactions.^[3–19] One typical type of heterogeneous catalysts for Suzuki coupling reactions is pure Pd nanoparticles.^[8–13] Since aryl halide is not soluble in water, the solvents widely used for Suzuki coupling reaction are organic solvent.^[1–3] Pd nanoparticles with small molecules as surfactants tend to aggregate in organic solvents at elevated temperature owing to the peeling off of the surfactants by organic solvents. The aggregation of Pd nanoparticles severely jeopardizes the catalytic performance. On the other hand, although Pd nanoparticles capped with relatively large molecular strand, for example oleic acid and polyvinylpyrrolidone, are

stable in organic solvent, the strong steric hinderance of surfactants greatly reduces the catalytic activity of Pd nanoparticles. The other type of heterogeneous catalysts is Pd atom, clusters, or nanoparticles anchored on supports.^[5–7,15,20] The supported Pd catalysts can exist stably without any surfactants and therefore effectively circumvent the reduction of catalytic activity induced by the aggregation and steric hinderance of surfactants.^[5–7,15,20]

Most of Suzuki coupling reactions takes place at thermal heating conditions, which consumes a relatively large amount of energy. To realize green Suzuki coupling reactions, Pd are integrated with solar active materials which absorb light to provide energy for reaction. For example, Au/Pd bimetallic nanoparticles have been utilized for photocatalytic Suzuki coupling reaction by use of the plasmon of Au nanoparticle.^[10–15] Pd nanoparticles have been loaded on SiC particles and achieved photocatalytic Suzuki coupling reaction.^[20] Similar to other two-dimensional materials,^[21,22] $g\text{-C}_3\text{N}_4$ has been widely studied in photocatalytic hydrogen evolution,^[23–25] CO_2 reduction^[26] and N_2 fixation^[27] owing to its suitable energy band structure, low cost, and facile synthesis. Moreover, compared with SiC, the abundant nitrogen atoms and six-fold cavities formed by nitrogen atoms can bind Pd nanoparticles or Pd atoms very strongly,^[6,23,25] which effectively inhibits the aggregation of Pd nanoparticles and thereby increases the stability.

Herein, by virtue of the light adsorption and the strong interaction with metal nanoparticles of $g\text{-C}_3\text{N}_4$, we prepared $g\text{-C}_3\text{N}_4$ supported Pd species ($g\text{-C}_3\text{N}_4/\text{Pd}$) for photocatalytic Suzuki coupling reactions. The catalytic efficiency of the catalyst under visible light irradiation is higher than those of the commercial tetrakis(triphenylphosphine)palladium ($\text{Pd}(\text{PPh}_3)_4$) and Pd nanocubes. The catalytic reactions carried out under different light power intensity show that the reaction is driven by the photo-generated hot electrons.

Compared with $g\text{-C}_3\text{N}_4$ prepared with other precursors, for example cyanamide and dicyandiamide, $g\text{-C}_3\text{N}_4$ prepared from urea has larger surface area and better dispersivity.^[28,29] We therefore employed urea as the source for the preparation of $g\text{-C}_3\text{N}_4$. Pd species was anchored on $g\text{-C}_3\text{N}_4$ by the sufficient mixing of H_2PdCl_4 with $g\text{-C}_3\text{N}_4$ and subsequent reduction of Pd. Figure 1 shows the X-ray diffraction (XRD) patterns of $g\text{-C}_3\text{N}_4$ and $g\text{-C}_3\text{N}_4/\text{Pd}$. Two prominent peaks appear at 12.8° and 27.4° , which are from the diffraction of (100) and (002) facets of $g\text{-C}_3\text{N}_4$.^[23,30,31] Besides these two peaks, other four peaks are present at 17.6° , 21.5° , 44.2° , and 56.8° , which are also observed in previous study.^[23,29] After loading Pd species, new diffraction peaks are observed at 39.8° , 45.9° , and 67.9° in the enlarged XRD pattern (Figure 1b), which are typical diffraction

N. Wang, L. X. Ma, J. Wang, Y. P. Zhang, Prof. R. B. Jiang
Key Laboratory of Applied Surface and Colloid Chemistry, National Ministry of Education
Shaanxi Key Laboratory for Advanced Energy Devices
Shaanxi Engineering Lab for Advanced Energy Technology
School of Materials Science and Engineering
Shaanxi Normal University
Xi'an 710119, China
E-mail: rbjiang@snnu.edu.cn

Supporting information for this article is given via a link at the end of the document.

from cubic phase Pd (JCPDS 05-0681). As a result, Pd nanoparticles are successfully anchored on $g\text{-C}_3\text{N}_4$.

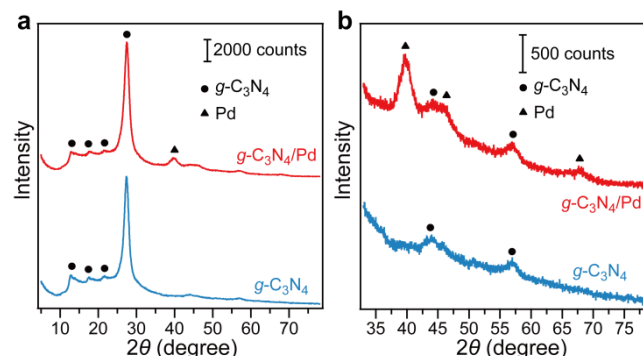


Figure 1. XRD patterns of $g\text{-C}_3\text{N}_4$ and $g\text{-C}_3\text{N}_4/\text{Pd}$. a) Full XRD patterns. b) Enlarged XRD patterns.

Figure 2a displays the transmission electron microscopy (TEM) image of $g\text{-C}_3\text{N}_4$. The $g\text{-C}_3\text{N}_4$ has relatively thin sheets, which is reflected by the low contrast of sample compared with region without sample. The Brunauer-Emmett-Teller characterization indicates that the specific surface area of the $g\text{-C}_3\text{N}_4$ is $72\text{ m}^2\text{ g}^{-1}$ (Figure S1), which is much larger than that ($4.2\text{ m}^2\text{ g}^{-1}$) of $g\text{-C}_3\text{N}_4$ prepared from dicyandiamide.^[23] These results are consistent with the previous studies that $g\text{-C}_3\text{N}_4$ prepared from urea has thin layers and very large surface area.^[23,28,29] Figure 2b shows the TEM image of $g\text{-C}_3\text{N}_4/\text{Pd}$. Tiny Pd nanoparticles can be observed. The distribution of the Pd nanoparticles is relatively uniform. The Pd nanoparticles can be more clearly observed in the TEM image with large magnification (Figure 2c). The average size of the Pd nanoparticles is $3.9 \pm 0.4\text{ nm}$. Such small nanoparticles make more Pd atoms exposed at surface and therefore improve the utilization efficiency of Pd. Moreover, the tiny nanoparticles increase the number of the low coordinated Pd atoms at surface. Therefore, the $g\text{-C}_3\text{N}_4/\text{Pd}$ should have very high catalytic activity for Suzuki coupling reactions.

High resolution TEM (HRTEM) was further carried out on $g\text{-C}_3\text{N}_4/\text{Pd}$. Clear lattice fringes can be observed on the nanoparticles, indicating the high crystallinity of the nanoparticles. The spacing between the lattice fringes is 0.224 nm , which corresponds to the spacing of $\{111\}$ facets of Pd. We also performed elemental mapping on $g\text{-C}_3\text{N}_4/\text{Pd}$. N and C distribute uniformly in the whole region (Figure S2a–c). The intensity of Pd signal is strong in the nanoparticle regions (Figure S2d), indicating that the nanoparticles are Pd nanoparticles. Besides the nanoparticle regions, Pd signal is also observed in the region without nanoparticles (Figure S2d). This indicates that, besides Pd nanoparticles, Pd may also exist as Pd cluster or single atoms on $g\text{-C}_3\text{N}_4$.

To confirm the chemical composition and state, we performed X-ray photoelectron spectroscopy (XPS) on $g\text{-C}_3\text{N}_4$ and $g\text{-C}_3\text{N}_4/\text{Pd}$. From the wide XPS spectra (Figure S3), only peaks related to N, C, and O are observed in $g\text{-C}_3\text{N}_4$. The presence of O may arise from the adsorption of adventitious

oxygen-containing species. Besides N, C, and O, Pd peaks are observed in $g\text{-C}_3\text{N}_4/\text{Pd}$ (Figure S3). Further analysis shows that the loading of Pd has negligible effect on the XPS spectra of C and N (Figure S4), indicating that the loading of Pd does not

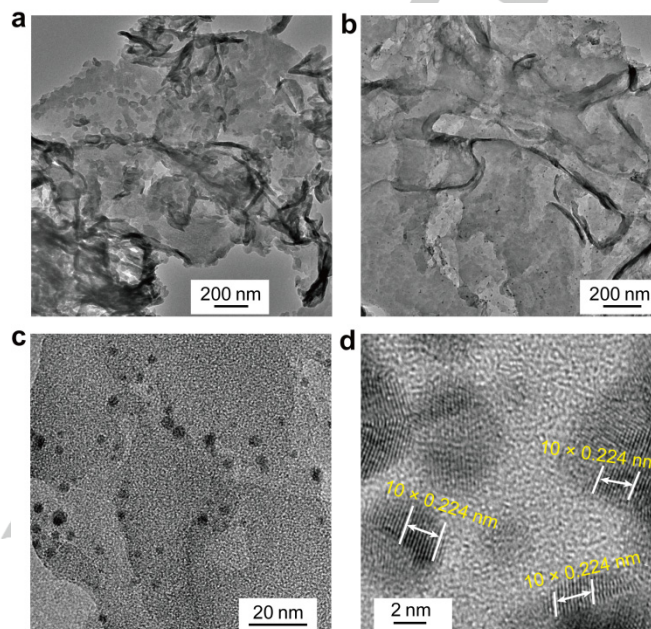


Figure 2. TEM images of $g\text{-C}_3\text{N}_4$ and $g\text{-C}_3\text{N}_4/\text{Pd}$. a) TEM image of $g\text{-C}_3\text{N}_4$. b,c) TEM images of $g\text{-C}_3\text{N}_4/\text{Pd}$ with low and high magnifications. d) HRTEM image of $g\text{-C}_3\text{N}_4/\text{Pd}$.

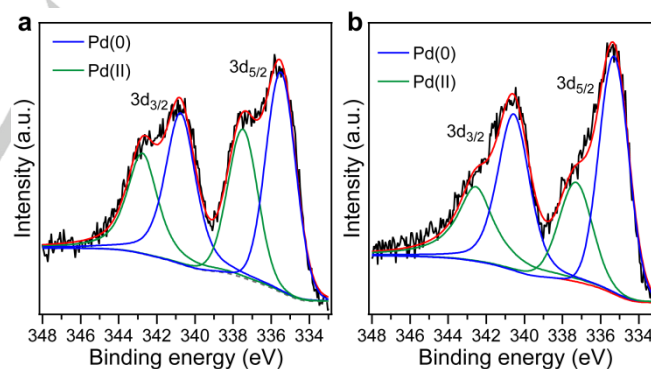


Figure 3. a) XPS of Pd 3d electrons in $g\text{-C}_3\text{N}_4/\text{Pd}$. b) XPS of Pd 3d electrons in $g\text{-C}_3\text{N}_4/\text{Pd-H}$.

break $g\text{-C}_3\text{N}_4$ structure. Figure 3a displays the fine XPS spectra of Pd 3d electrons in $g\text{-C}_3\text{N}_4/\text{Pd}$. Four peaks are present at 342.8 eV , 340.8 eV , 337.5 eV , and 335.5 eV . Two peaks at high binding energy are corresponding to Pd $3d_{3/2}$, while the other two peaks are related to Pd $3d_{5/2}$. The peaks at 335.5 eV and 340.8 eV correspond to Pd(0),^[32] which should from Pd nanoparticles. The peaks at 337.5 eV and 342.8 eV correspond to Pd(II).^[32] The presence of Pd(II) may arise from the surface oxidation Pd nanoparticles or from the doping of single Pd ions in the six-fold cavities of $g\text{-C}_3\text{N}_4$.^[6,23,26] If the former is true, the

Pd(II) peaks would disappear after H₂ reduction because it can be effectively convert Pd(II) into Pd(0). Thereupon, we carried XPS characterization on the H₂-reduced *g*-C₃N₄/Pd (*g*-C₃N₄/Pd-H). After reduced with H₂, the Pd(II) peaks are obviously weakened but still have relatively strong intensity, indicating that Pd(II) is from both the surface oxidation of Pd nanoparticles and the doping of single Pd atoms. The existence of Pd(II) in six-fold cavities of *g*-C₃N₄ is consistent with the elemental mapping results that Pd distributes in the whole *g*-C₃N₄. Indeed, Pd can stably exist as single atoms in the six-fold cavities of *g*-C₃N₄.^[6,23,26] Based on the above characterizations, we can conclude that Pd exists on *g*-C₃N₄ as nanoparticles and single Pd atoms.

The content of Pd of *g*-C₃N₄/Pd was determined by energy-dispersive X-ray (EDX) and inductively coupled plasma optical emission spectrometry (ICP-OES) (Figure S5). EDX analysis shows the Pd content of 1.9 wt.%, which is very close the value (1.5 wt.%) obtained from ICP-OES. In the following turnover frequency (TOF) calculation, the ICP-OES result is used. Coupling reaction between iodobenzene and phenylboronic acid was utilized to study the photocatalytic performance of *g*-C₃N₄/Pd (Figure 4a). Figure 4b shows the conversion of iodobenzene under different reaction conditions. Under light illumination ($\lambda > 400$ nm), *g*-C₃N₄ shows no photocatalytic activity for the coupling reaction. In contrast, *g*-C₃N₄/Pd gives rise to a conversion of 100% for iodobenzene within 45 min under light illumination, which is very close to the conversion obtained under thermal heating of 78 °C. This indicates that *g*-C₃N₄/Pd is an excellent photocatalyst for Suzuki coupling reactions. Without the light illumination and thermal heating, the conversion of iodobenzene decreases to 39.3% in the presence of *g*-C₃N₄/Pd. Moreover, nearly the same iodobenzene conversion is obtained on *g*-C₃N₄/Pd-H, indicating that the H₂ reduction has negligible effect on the photocatalytic activity of *g*-C₃N₄/Pd.

conversion of iodobenzene at 405 nm. e) Recyclability of *g*-C₃N₄/Pd for photocatalytic Suzuki coupling reactions.

The photocatalytic performance of *g*-C₃N₄/Pd for Suzuki coupling reaction was further studied at the illumination of light with different wavelengths (Table S1). The conversion of iodobenzene has the same trend as the absorption of light by the *g*-C₃N₄/Pd (Figure 4c), indicating the reaction is driven by the light. One should point out that the band-gap of *g*-C₃N₄ is 2.75 eV (Figure S6), while *g*-C₃N₄/Pd exhibit photocatalytic activity in the whole visible region. This may arise from the electron excitation between *g*-C₃N₄ and inset single Pd ions in the cavities of *g*-C₃N₄, which gives rise to absorption in the wavelength longer than the band-gap of *g*-C₃N₄.^[23,33] At the fixed light wavelength of 405 nm, the conversion of iodobenzene catalyzed by *g*-C₃N₄/Pd exhibits an almost linear increase with the increase of light intensity (Figure 4d and Table S2). The conversion of iodobenzene without light irradiation results from the thermal contribution. By subtracting the thermal contribution, the light contribution is obtained. It can be seen that, as the light intensity is increased, the light contribution is greater. It has been demonstrated that the linear dependence of reaction conversion on the light intensity is a signature of an electron-driven chemical process.^[15,34] As a result, the reaction catalyzed by *g*-C₃N₄/Pd under light irradiation is driven by photo-excited electrons of *g*-C₃N₄. In addition, the *g*-C₃N₄/Pd displays very good recyclability for Suzuki coupling reactions (Figure 4e). The slight decrease of performance may arise from the inevitable loss of catalyst during centrifugation. After three cycles, the *g*-C₃N₄/Pd does not any observable changes (Figure S7).

The photocatalytic performance of *g*-C₃N₄/Pd was further compared with Pd nanocubes (Figure S8) and Pd(PPh₃)₄. During the catalysis, the amount of Pd is kept the same for all three catalysts. The reaction condition is kept the same except that the reaction catalyzed by Pd(PPh₃)₄ is carried out at thermal heating of 78 °C. Figure 5a shows the conversion of iodobenzene catalyzed by *g*-C₃N₄/Pd, Pd nanocubes, and Pd(PPh₃)₄. At the same reaction time, the conversion of reaction catalyzed by *g*-C₃N₄/Pd is almost two times of that catalyzed by Pd(PPh₃)₄. The conversion of the reaction catalyzed by Pd nanocubes is slightly smaller than that catalyzed by Pd(PPh₃)₄. The corresponding TOFs of the three catalysts are shown in Figure 5b. The TOF of *g*-C₃N₄/Pd is 47.3 h⁻¹, which is much larger than those of Pd(PPh₃)₄ and Pd nanocubes. This clearly indicates that *g*-C₃N₄/Pd is an excellent photocatalyst for Suzuki coupling reaction with TOF surpassing that of commercial Pd(PPh₃)₄ catalyst under thermal heating.

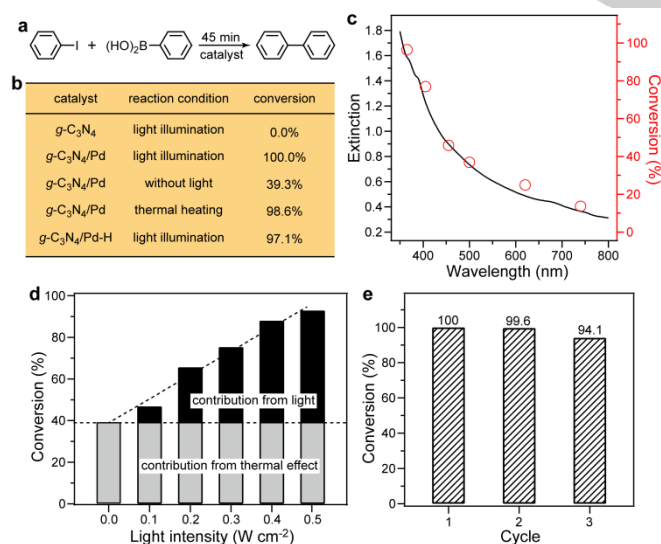


Figure 4. Photocatalytic Suzuki coupling reaction. a) Reaction formula. b) Conversions of iodobenzene at different catalytic conditions. The light source is a 300 W xenon lamp equipped with a 400 nm long-pass filter. c) Wavelength-dependent conversion of iodobenzene. d) Power-dependent

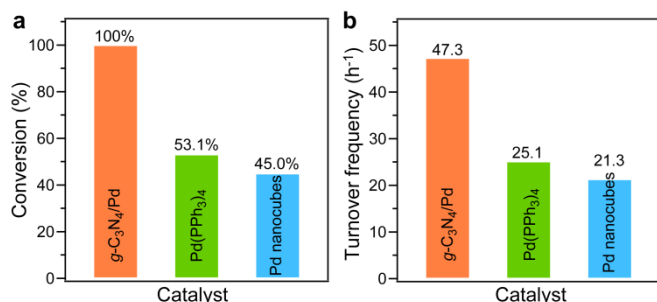


Figure 5. a) Conversion of iodobenzene catalyzed by different catalysts within 45 min. b) TOF of different catalysts. The TOF is calculated on the basis of all Pd atoms.

To study the application of the *g*-C₃N₄/Pd catalyst, more Suzuki reactions between different arylhalide and phenylboronic acid or its derivatives were carried out under light irradiation. This catalyst exhibits excellent performance towards the studied substrates (Table 1). For iodobenzene and phenylboronic acid and their derivatives (Table 1, Entries 1–6), the conversions are all higher than 90%, and the TOFs are all larger than 40 h⁻¹. Importantly, by elongating the reaction time to 90 min, the conversion of bromobenzene can also reach 90.0%, and the TOF is 21.3 h⁻¹ (Table 1, Entry 7). Hence, the *g*-C₃N₄/Pd is a very good universal photocatalysis for Suzuki coupling reactions.

Table 1. Suzuki reactions with different substrates over *g*-C₃N₄/Pd under light illumination^a

Entry	Aryl halides	Boronic acids	Conversion (%)	TOF (h ⁻¹)
1			~100	47.3
2			98.3	46.4
3			89.6	42.4
4			99.0	46.8
5			98.9	46.8
6			98.7	46.7
7			90.0	21.3

[a] Reaction conditions: 0.15 mmol of aryl halides, 0.225 mmol of aryl boronic acid, 50 mg of *g*-C₃N₄/Pd, 1 mmol of K₂CO₃, 5 mL of solvent, under air, reaction time of 45 min for aryl iodide and of 90 min for bromobenzene. The light source is a 300 W xenon lamp equipped with a 400 nm long-pass filter. The TOF is calculated on the basis of all Pd atoms.

In summary, we have successfully prepared *g*-C₃N₄/Pd and studied its photocatalytic performance for Suzuki coupling reactions. The *g*-C₃N₄/Pd is prepared through the reduction of Pd source in the presence of *g*-C₃N₄. The Pd is found to exist as Pd nanoparticles and Pd(II) species on *g*-C₃N₄. Owing to the good light absorption of *g*-C₃N₄ and the excellent catalytic activity of Pd species, the *g*-C₃N₄/Pd exhibits an excellent

photocatalytic performance for Suzuki coupling reactions with TOF of 47.3 h⁻¹, which is almost two times of that of commercial homogeneous catalyst, Pd(PPh₃)₄, under thermal heating. Moreover, *g*-C₃N₄/Pd displays very good recyclability and wide applicability for Suzuki coupling reactions. Our findings provide a green and sustainable way for the catalysis of Suzuki coupling reactions.

Acknowledgements

N.W. and L.X.M. contributed equally to this work. This work was supported by the National Natural Science Foundation of China (61775129), the 111 Project (B14041), Fundamental Research Funds for the Central Universities (GK201902001), Funded Projects for the Academic Leaders and Academic Backbones of Shaanxi Normal University (18QNGG008).

Keywords: graphitic carbon nitride • palladium • photocatalysis • nanostructures • Suzuki coupling

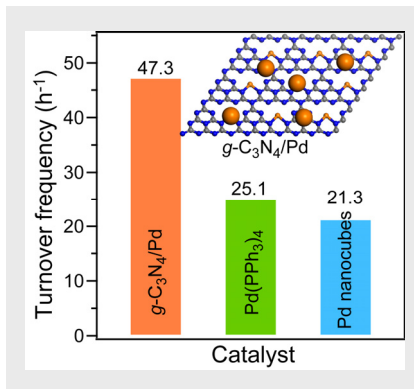
- [1] N. Miyaura, A. Suzuki, *Chem. Rev.* **1995**, *95*, 2457–2483.
- [2] R. Chinchilla, C. Nájera, *Chem. Rev.* **2007**, *107*, 874–922.
- [3] C. C. C. Johansson Seechurn, M. O. Kitching, T. J. Colacot, V. Snieckus, *Angew. Chem. Int. Ed.* **2012**, *51*, 5062–5085.
- [4] Á. Molnár, **2011**, *111*, 2251–2320.
- [5] X. Zhang, Z. Sun, B. Wang, Y. Tang, L. Nguyen, Y. Li, F. F. Tao, *J. Am. Chem. Soc.* **2018**, *140*, 954–962.
- [6] Z. Chen, E. Vorobyeva, S. Mitchell, E. Fako, M. A. Ortuño, N. López, S. M. Collins, P. A. Modgley, S. Richard, G. Vilé, J. Pérez-Ramírez, *Nat. Nanotechnol.* **2018**, *13*, 702–707.
- [7] Y. Yang, A. C. Reber, S. E. Gilliland, C. E. Castano, B. F. Gupton, S. N. Khanna, *J. Phys. Chem. C* **2018**, *122*, 25396–25403.
- [8] F. Wang, C. Li, L.-D. Sun, H. Wu, T. Ming, J. F. Wang, J. C. Yu, C.-H. Yan, *J. Am. Chem. Soc.* **2011**, *133*, 1106–1111.
- [9] F. Wang, C. Li, L.-D. Sun, C.-H. Xu, J. Wang, J. C. Yu, C.-H. Yan, *Angew. Chem. Int. Ed.* **2012**, *51*, 4872–4876.
- [10] F. Wang, C. Li, H. Chen, R. Jiang, L.-D. Sun, Q. Li, J. Wang, J. C. Yu, C.-H. Yan, *J. Am. Chem. Soc.* **2013**, *135*, 5588–5601.
- [11] X. Huang, Y. Li, Y. Chen, H. Zhou, X. Duan, Y. Huang, *Angew. Chem. Int. Ed.* **2013**, *52*, 6063–6067.
- [12] Y. X. Hu, Y. Z. Liu, Z. Li, Y. G. Sun, *Adv. Funct. Mater.* **2014**, *24*, 2828–2836.
- [13] Y. Li, E. Boone, M. A. El-Sayed, *Langmuir* **2002**, *18*, 4921–4925.
- [14] Q. Xiao, S. Sarina, E. Jaatinen, J. F. Jia, D. P. Arnold, H. W. Liu, H. Y. Zhu, *Green Chem.* **2014**, *16*, 4272–4285.
- [15] S. Sarina, H. Zhu, E. Jaatinen, Q. Xiao, H. Liu, J. Jia, C. Chen, J. Zhao, *J. Am. Chem. Soc.* **2013**, *135*, 5793–5801.
- [16] S.-W. Kim, M. Kim, W. Y. Lee, T. Hyeon, *J. Am. Chem. Soc.* **2002**, *124*, 7642–7643.
- [17] A. Suzuki, *J. Organomet. Chem.* **1999**, *576*, 147–168.
- [18] G. P. Roth, V. Farina, L. S. Liebeskind, E. Peña-Cabrera, *Tetrahedron Lett.* **1995**, *36*, 2191–2194.
- [19] P. Mondal, P. Bhanja, R. Khatun, A. Bhaumik, D. Das, S. M. Islam, *J. Colloid Interface Sci.* **2017**, *508*, 378–386.
- [20] Z. Jiao, Z. Zhai, X. Guo, X.-Y. Guo, *J. Phys. Chem. C* **2015**, *119*, 3238–3243.
- [21] S. Wang, Z. Li, Y. Zhang, X. Liu, J. Han, X. Li, Z. Liu, S. Liu, W. C. H. Choy, *Adv. Funct. Mater.* **2019**, *29*, 1900417.
- [22] X. Li, S. Guo, W. Li, X. Ren, J. Su, Q. Song, A. J. Sobrido, B. Wei, *Nano Energy* **2019**, *57*, 388–397.
- [23] N. Wang, J. Wang, J. H. Hu, X. Q. Lu, J. Sun, F. Shi, Z.-H. Liu, Z. B.

- Lei, R. B. Jiang, *ACS Appl. Energy Mater.* **2018**, *1*, 2866–2873.
- [24] S. W. Cao, J. X. Low, J. G. Yu, M. Jaroniec, *Adv. Mater.* **2015**, *27*, 2150–2176.
- [25] Q. Han, Z. H. Cheng, B. Wang, H. M. Zhang, L. T. Qu, *ACS Nano* **2018**, *12*, 5221–5227.
- [26] G. P. Gao, Y. Jiao, E. R. Waclawik, A. J. Du, *J. Am. Chem. Soc.* **2016**, *138*, 6292–6297.
- [27] C. Y. Ling, X. H. Niu, Q. Li, A. J. Du, J. L. Wang, *J. Am. Chem. Soc.* **2018**, *140*, 14161–14168.
- [28] Y. Z. Guo, H. L. Jia, J. H. Yang, H. Yin, Z. Yang, J. F. Wang, B. C. Yang, *Phys. Chem. Chem. Phys.* **2018**, *20*, 22296–22307.
- [29] F. Dong, Z. W. Zhao, T. Xiong, Z. L. Ni, W. D. Zhang, Y. J. Sun, W.-K. Ho, *ACS Appl. Mater. Interfaces* **2013**, *5*, 11392–11401.
- [30] Y. Wang, X. C. Wang, M. Antonietti, *Angew. Chem. Int. Ed.* **2012**, *51*, 68–89.
- [31] X. C. Wang, K. Maeda, A. Thomas, K. Takane, G. Xin, J. M. Carlsson, K. Domen, M. Antonietti, *Nat. Mater.* **2009**, *8*, 76–80.
- [32] J. F. Moulder, W. F. Stickle, P. E. Sobol, K. D. Bomben, *Handbook of X-Ray Photoelectron Spectroscopy*, (Edit.: J. Chastain), Perkin-Elmer Corporation, USA, **1992**.
- [33] Y. Li, Z. Wang, T. Xia, H. Ju, K. Zhang, R. Long, Q. Xu, C. Wang, L. Song, J. Zhu, J. Jiang, Y. Xiong, *Adv. Mater.* **2016**, *28*, 6959.
- [34] P. Christopher, H. L. Xin, S. Linic, *Nat. Chem.* **2011**, *3*, 467–472.

Entry for the Table of Contents (Please choose one layout)

COMMUNICATION

$g\text{-C}_3\text{N}_4/\text{Pd}$ is successfully prepared for photocatalytic Suzuki coupling reactions. The TOF of $g\text{-C}_3\text{N}_4/\text{Pd}$ for Suzuki coupling reaction under visible light irradiation is up to 47.3 h^{-1} , which is almost two times of that of commercial homogeneous catalyst, $\text{Pd}(\text{PPh}_3)_4$, under thermal heating.



Nan Wang, Lixia Ma, Jing Wang, Yanpei Zhang, and Ruibin Jiang*

Page No. – Page No.

Graphitic Carbon Nitride ($g\text{-C}_3\text{N}_4$) Supported Pd Species: An Efficient Heterogeneous Photocatalyst Surpassing Homogeneous Thermal Heating Systems for Suzuki Coupling